RESEARCH FRONT

Research Paper

CSIRO PUBLISHING

A. Iijima et al., *Environ. Chem.* **2009**, *6*, 122–132. doi:10.1071/EN08107 www.publish.csiro.au/journals/env

Clarification of the predominant emission sources of antimony in airborne particulate matter and estimation of their effects on the atmosphere in Japan

Akihiro Iijima,[A,B,F] *Keiichi Sato*,[C] *Yuji Fujitani*,[D] *Eiji Fujimori*,[E] *Yoshinori Saito*,[A] *Kiyoshi Tanabe*,[D] *Toshimasa Ohara*,[D] *Kunihisa Kozawa*[A] *and Naoki Furuta*[B]

[A]Gunma Prefectural Institute of Public Health and Environmental Sciences, 378 Kamioki, Maebashi, Gunma 371-0052, Japan.

[B]Faculty of Science and Engineering, Department of Applied Chemistry, Chuo University, 1-13-27 Kasuga, Bunkyo-ku, Tokyo 112-8551, Japan.

[C]Data Management Department, Acid Deposition and Oxidant Research Center, 1182 Sowa, Nishi-ku, Niigata 950-2144, Japan.

[D]National Institute for Environmental Studies, 16-2 Onogawa, Tsukuba, Ibaraki 305-8506, Japan.

[E]National Environmental Research and Training Institute, 3-3 Namiki, Tokorozawa, Saitama 359-0042, Japan.

[F]Corresponding author. Email: iijima-akihiro@pref.gunma.jp

Environmental context. The remarkable enrichment of potentially toxic antimony (Sb) in inhalable airborne particulate matter has become of great environmental concern among recent air pollution issues. The present study clarifies the predominant sources of Sb by focusing on the similarities in elemental composition, particle size distributions, and microscopic images found in ambient airborne particles and several potential sources. We identify automotive brake abrasion dust and fly ash emitted from waste incineration as dominant sources of atmospheric Sb in Japan. These results will contribute towards an in-depth understanding of the cycles and fates of Sb in the environment.

Abstract. By focusing on the similarities in elemental composition, particle size distributions of elemental concentrations, and microscopic images between ambient airborne particulate matter (APM) and several potential sources, we discuss the predominant sources of antimony (Sb) in APM in Japan. The distribution of Sb concentration in size-classified ambient APM showed a characteristic bimodal profile in which peaks were found in coarse (3.6–5.2 μm) and fine (0.5–0.7 μm) fractions. Elemental ratios, particle sizes, and microscopic images observed in the coarse APM fractions were found to be in good agreement with those of brake abrasion dust. However, in the fine APM fractions, fly ash originating from waste incineration was identified as the most probable source of Sb. Chemical mass balance analysis was performed to determine the effects of the emission sources of Sb, and it was revealed that brake abrasion dust and waste fly ash were the dominant sources of Sb in the coarser and the finer fractions of APM, respectively. The present study provides important clues to understanding the cycles and fates of Sb in the environment.

Additional keywords: brake abrasion dust, elemental ratio, microscopic image, particle size distribution, waste fly ash.

Introduction

Antimony (Sb) and its compounds possess useful applications, such as being semi-metallic, flame-proofing, and acting as a hardener in lead. Hence, they have been widely used in functional materials. Nevertheless, awareness regarding the negative effect of such compounds on the environment and ecosystem has arisen. However, to date, the environmental effects, the material cycles, and the fates of potentially toxic Sb compounds have not been sufficiently studied compared with those of As, Hg, and Cd.[1–3] The analyses of samples of environmental archives such as peat layers and ice cores have revealed significant changes in the concentrations of various atmospheric pollutants, which are possibly due to the drastic changes in human activities after the Second Industrial Revolution.[4] These historical records have revealed that the temporal trend of the anthropogenic effect of Sb on the environment between the mid- and late 20th century was strongly dominated by two major emission sources – coal combustion and metallurgical processes.[4–8] These effects, derived from the deposition of airborne particulate matter (APM), have originated from the aforementioned human activities. Indeed, coal combustion and metallurgical processes have been pointed out as potential sources of Sb in APM collected in the mega-city of Shanghai, China.[9,10] Pacyna and Pacyna[11] estimated the total anthropogenic emissions of Sb, Cr, Hg, Mn, Se, Sn, and Tl into the atmosphere from individual anthropogenic emission sources. The total Sb emission was estimated to be 1561 tonnes per year in the mid-1990s. In their estimation, stationary fossil fuel combustion (mainly coal combustion) and non-ferrous metal production were found to be the dominant sources of Sb emission. Interestingly, during the past few decades another

1448-2517/09/020122

remarkable enrichment of Sb has been observed from peat layer and ice core samples, implying the emergence of new anthropogenic Sb sources.[6,7] This emergence is most likely to be related with the recent expansion of Sb applications to functional materials, such as flame retardants for plastics and chemical fabrics and lubricants for automotive brake friction materials.

Our recent studies have demonstrated that APM collected at the centre and in the suburbs of Tokyo, Japan, are extremely enriched with Sb.[12,13] Similar results were obtained in various other countries such as the USA,[14] Germany,[15] and Argentina.[16] Automotive brake abrasion dusts have been commonly pointed out as one of the important Sb sources. Therefore, we have evaluated the particle size distribution and elemental composition of brake abrasion dusts and the emission processes of dusts to the atmosphere in detail.[17,18] The results have confirmed that automotive brake abrasion dust significantly influences the enrichment of Sb in APM. Moreover, the emission of Sb from automotive brake pads was estimated to be 21 tonnes per year in Japan in 2000, implying that brake abrasion dust could be an important source of Sb in roadside environments. However, the temporal trend of substance flow of Sb compounds in Japan indicates that the domestic supplies of Sb compounds began to increase significantly towards the beginning of the 21st century owing to the increase in use of Sb as a flame retardant for plastic products used in electric appliances, information technology (IT) and office automation (OA) devices, etc.[19] Because a part of household wastes containing plastic products is incinerated in Japan, Sb emission from incineration plants may have increased accordingly. Therefore, fly ash originating from waste incineration may be another important Sb source in Japan. From a global perspective, Sb emission from waste incinerators has been highlighted as a major factor for pollution after those originating from fossil fuel combustion and non-ferrous metal production.[11]

Hence, a quantitative evaluation of the magnitude and effects of potential Sb sources on the atmosphere is required for an in-depth understanding on the confronting concerns regarding the enrichment of Sb in the environment. Metallic elements present in environmental samples are considered to be excellent fingerprints that indicate the origins of the samples.[20] In particular, some trace elements play an important role in indicating the origin of samples.[13] In the present study, size-classified ambient APM samples were collected at two different locations: a roadside site and a residential site, and multielement analysis was performed in order to determine the definitive fingerprints of potential sources of Sb in APM. In addition, microscopic observation was carried out to clarify the morphological features of Sb-containing particles. Meanwhile, to develop the database used for qualitative and quantitative identification of atmospheric Sb sources, multidimensional source profiling consisting of the determination of elemental composition, measurement of particle size distribution, and imaging of individual particles was carried out for several potential APM sources. By focusing on the similarities in elemental composition, particle size, and microscopic images between the ambient APM and several potential sources, the effects of predominant emission sources of Sb in APM are discussed.

Experimental

Collection of size-classified ambient APM

Sample collection of size-classified APM was performed at a roadside site (Tatebayashi: 36.2°N, 139.5°E, ~20 m above sea level – ASL) and a residential site (Maebashi: 36.4°N, 139.1°E, ~130 m ASL). The roadside site is located at the intersection of the heavy traffic-carrying national highways 122 and 354. During weekdays, the average traffic density is estimated to be ~40 000 vehicles per day. Extraordinary traffic jams frequently occur during morning and evening rush hours. The residential site is located in a small city (population 0.3 million) in a northwestern suburban area situated 100 km away from the centre of Tokyo and 50 km west away from the roadside site. The sampling periods ranged from 2 to 5 September 2008 for the roadside site, and from 28 August to 2 September 2008 for the residential site. Sample collection in both the sites was conducted under typical meteorological conditions during summer time in Japan (high temperature and humidity conditions; average temperature 25°C; average relative humidity 75%). Thirteen fractions of size-classified APM (with aerodynamic diameter $D\mathrm{p} < 0.06$, 0.06–0.12, 0.12–0.20, 0.20–0.30, 0.30–0.50, 0.50–0.70, 0.70–1.2, 1.2–2.1, 2.1–3.6, 3.6–5.2, 5.2–7.9, 7.9–11, and >11 μm) were collected on cellulose acetate membrane filters (Toyo Roshi Kaisha Ltd, Tokyo, Japan) using an Andersen-type Low Pressure Impactor (LPI) air sampler (LP-20; Tokyo Dylec Co., Tokyo, Japan).

To compare the effect of vehicular traffic between both the sites, concentrations of NO and NO_2 were continuously monitored using a nitrogen oxides analyser with a chemiluminescence detector (GPH-74M-1; DKK-TOA Co., Tokyo, Japan). The average concentrations of NO and NO_2 during the sampling periods were determined to be 24 and 22 parts per billion by volume (ppbv) for the roadside site and 2 and 11 ppbv for the residential site, respectively. A relatively high concentration of NO, a marker component of primary automobile emission, was observed at the roadside site, indicating that the vehicular traffic had a significant effect on the atmosphere around the roadside site.

Collection of dust samples from potential sources

Dust samples were collected from six types of typical emission sources of APM in Japan (see Table 1). Six of 10 waste fly ash samples were collected on silica glass microfibre filters (Whatman International Ltd, Maidstone, England) from flues of different incinerators according to the procedure prescribed in the Japan Industry Standard (JIS) Z 8808. The remaining four waste fly ash samples were collected from electric precipitators in different incinerators, and they were stored in glass vials for the measurement of particle size distribution. Fly ash samples from heavy oil combustion (oil fly ash; eight samples) and wood combustion (wood fly ash; three samples) were collected from flues of different boilers following a procedure (JIS Z 8808) identical to that described above. Similarly, diesel exhaust particle (DEP) samples from heavy oil combustion (three samples) were collected from flues of electricity generators. Soil samples (three samples) were collected from the surface layers of bare ground in typical urban and suburban areas. After desiccation, the soil samples were filtered through a 40-μm sieve. Brake abrasion dust samples (three samples) were generated by friction of brake pads and a cast iron disk that were installed in a brake dynamometer. Detailed descriptions of a full-size brake dynamometer system and the sample collection procedures have been provided in our previous studies.[17,18] As described previously, coal combustion is estimated as one of the important sources of Sb from a global perspective.[11] To elucidate the effect of coal combustion, we obtained the standard reference material SRM 2689 (coal fly ash) prepared by the US National Institute of Standards and Technology (NIST, Gaithersburg, MD, USA) in addition to the

Table 1. Collection resources of dust samples from typical emission sources of airborne particulate matter (APM) in Japan

Potential source	Fuel or origin	Sampling point	Sample number
Waste fly ash	Household and industrial waste	Incinerator/electric precipitator or flue	10
Oil fly ash	Heavy oil	Boiler/flue	8
Wood fly ash	Scrap wood	Boiler/flue	3
Diesel exhaust particle (DEP)	Heavy oil	Electricity generator/flue	3
Soil	Surface soil	Bare ground/surface layer	3
Brake abrasion dust	Brake pad	Passenger vehicle/brake dynamometer	3

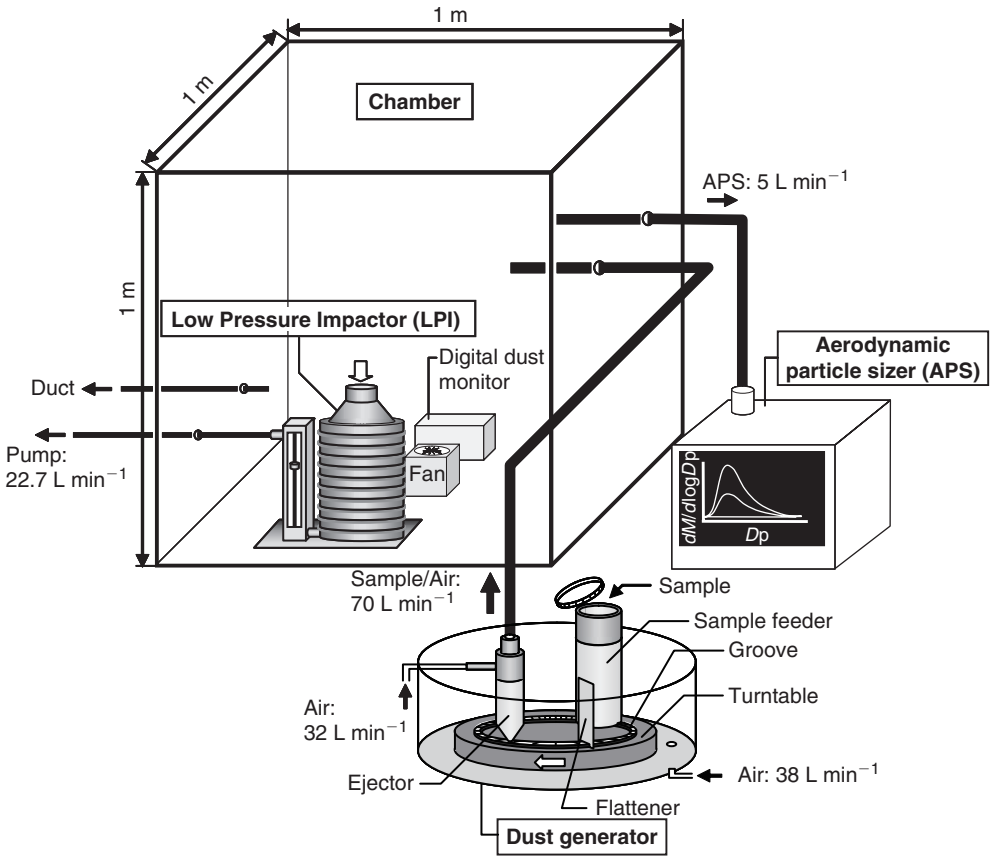

Fig. 1. Instrumental layout for re-entrainment examination of waste fly ash.

samples collected from the aforementioned six types of emission sources.

Re-entrainment examination of waste fly ash

Clarification of the particle size distribution of dust samples is expected to enhance the reliability of source identification. According to the substance flow analysis of Sb in Japan, automotive brake abrasion dusts and waste fly ashes are expected to be the major sources of Sb in APM.[19] As mentioned above, particle size distribution of brake abrasion dusts has been evaluated in detail in our previous studies.[17] In the present study, therefore, particle size distribution and elemental distribution in size-classified dust samples were investigated for a selected waste fly ash sample by re-entrainment examination, described as follows.

An LPI sampler and a digital dust monitor (LD-3; Sibata Scientific Technology Ltd, Tokyo, Japan) were installed in an enclosed chamber ($1 \times 1 \times 1$ m) made from antistatic-finished polyvinyl chloride sheets (see Fig. 1). A dust generator (DF-3; Sibata Scientific Technology Ltd) was connected to the chamber. An adequate amount of desiccated fly ash sample was placed into the sample feeder, and it was intermittently supplied into grooves laid on a turntable. Then, the samples placed in the grooves were intermittently sucked up by a dehumidified air flow into an ejector, and they were finally scattered into the chamber and well mixed by a fan. The concentration of dust in the chamber was measured by a digital dust monitor, and it was controlled to be $\sim$1 mg m^{-3} by varying the revolving speed of the turntable. Size-classified dust samples were collected on Polyflon filters (PF 060 for impaction stages, PF 020 for the backup stage; Toyo Roshi Kaisha Ltd) using an LPI sampler, and the particle size distribution was monitored using an aerodynamic particle sizer (APS) spectrometer (Model 3321 APS, TSI Inc., Shoreview, MN, USA) in order to confirm emission of dusts for respective size fractions. Because excessive air flow was naturally released through a duct, the inner pressure was maintained at atmospheric pressure.

Chemical analysis

Half of the pieces of the sample-loaded filters collected at the roadside site and the residential site were digested in a mixture of 2 mL of hydrofluoric acid (50% atomic absorption spectrometry (AAS) grade, Kanto Chemical Co. Inc., Tokyo, Japan), 5 mL of nitric acid (60% ultrapure chemicals), and 1 mL of hydrogen peroxide (30% AAS grade) in a microwave digestion system (Multiwave, Anton Paar GmbH, Graz, Austria) under the conditions of 700 W for 10 min and 1000 W for a further 10 min. Hydrofluoric acid was evaporated by heating the sample solution at 200°C on a hot plate, and 0.1 mol L^{-1} nitric acid (prepared from 60% nitric acid) was then added to obtain a 50-mL sample. Likewise, half of the pieces of the sample-loaded filters collected from the re-entrainment examination were digested by an identical procedure. Adequate amounts (several tens of grams) of fly ash, DEP, or soil samples were digested by an identical procedure, and the digested solutions were further diluted 100-fold with 0.1 mol L^{-1} nitric acid. The concentrations of trace elements such as V, Cr, Mn, Ni, Cu, Zn, As, Se, Mo, Cd, Sb, Ba, and Pb in the final solutions were determined by inductively coupled plasma mass spectrometry (Agilent 7500cx, Agilent Technologies Inc., Tokyo, Japan). Descriptions of the analytical procedures employed for brake abrasion dust samples have been provided in our previous studies.[17,18] All the analytical procedures were validated by using the SRM 1648 (urban particulate matter) prepared by NIST. The analytical results are listed in the Appendix. They showed good agreement with the certified or reference values.

Microscopic observation

To characterise the microscopic fingerprints of Sb-enriched APM, the particle shapes and elemental distributions were measured using a scanning electron microscope (SEM) (S-5500, Hitachi High-Technologies Co., Tokyo, Japan) equipped with an energy-dispersive X-ray spectroscopic detector (EDX) (EMAX; Horiba Ltd, Kyoto, Japan). The imaging analysis of elemental distribution was performed using characteristic X-ray spectra for elements obtained with an acceleration voltage of 30 kV.

Results and discussion

Overview of the distributions of elemental concentrations in size-classified ambient APM

Fig. 2 shows the size distributions and elemental concentrations for Sb, Cu, Ba, Cd, and Pb in size-classified ambient APM collected at the roadside and residential sites.

At the roadside site, the total mass concentration of Sb was 3.7 ng m^{-3} (it must be noted that the *y* axis in Fig. 2 has a scale of $dM/d\log Dp$, where *M* is mass concentration), and the size distribution of Sb concentration exhibits a bimodal profile in which peaks are found in the coarse (3.6–5.2 μm) and the fine (0.5–0.7 μm) fractions. This bimodal profile of Sb is unique

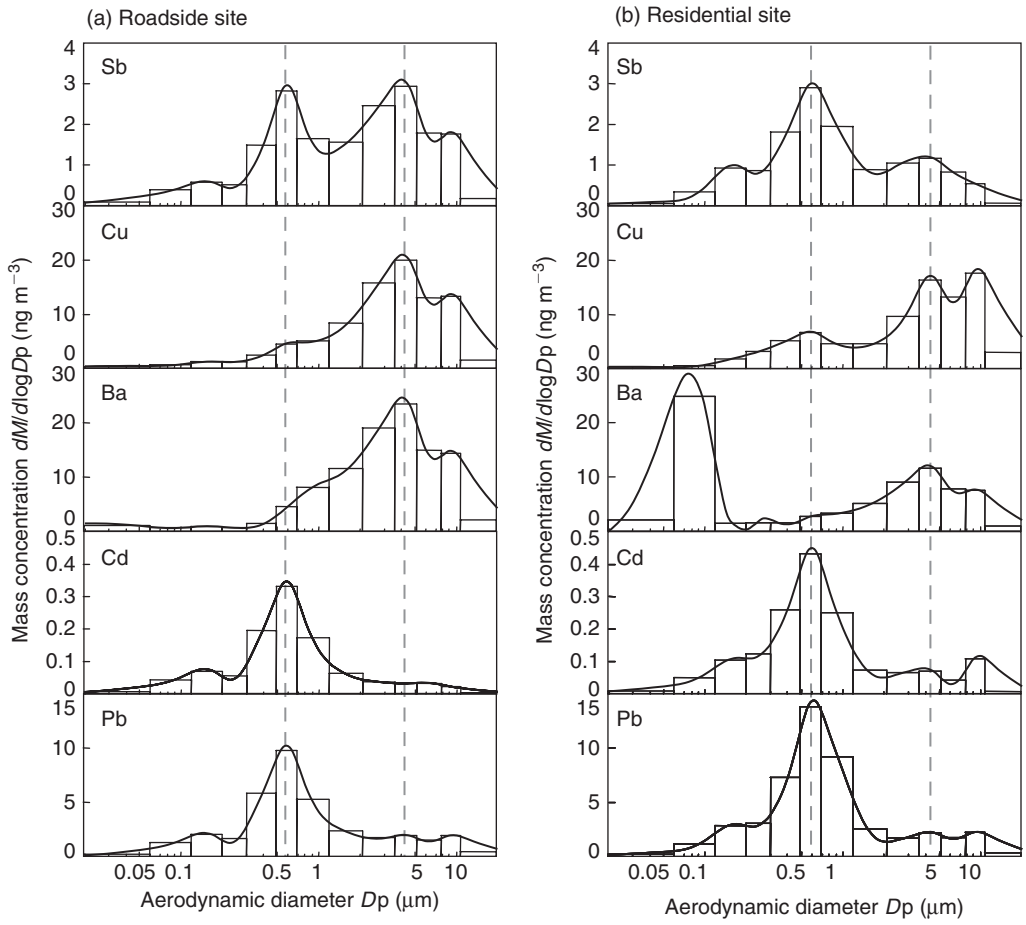

Fig. 2. Distributions of elemental concentration in size-classified airborne particulate matter (APM) collected at (a) the roadside site and (b) the residential site. The solid curve indicates a smoothed distribution and the broken lines indicate the coarser and finer peak diameters in Sb distribution.

among those of the 13 elements measured in the current study. The distribution of Sb in coarse fractions is highly similar to those observed in Cu and Ba, whereas the distribution of Sb in fine fractions is highly similar to those in Cd and Pb. For the other elements, no specific distribution related to Sb was observed.

At the residential site, the total mass concentration of Sb was 2.7 ng m^{-3}, which is relatively lower than that observed at the roadside site. Although the peaks in the Sb distribution were found to be the same in both the coarse (3.6–5.2 μm) and the fine (0.5–0.7 μm) fractions as those in the roadside site, the coarser fraction peak was considerably smaller than that found in the roadside site distribution. Again, the distribution of Sb in coarse fractions was broadly similar to those observed in Cu and Ba, whereas the size distribution of Sb in fine fractions was highly similar to those of Cd and Pb as well as at the roadside site. In the elemental distribution of Ba, the prominent peak was observed in the nano-sized fraction. We confirmed this observation by several repeated experiments. This suggests that there were some unknown sources of Ba-containing nano-sized particles around the site.

In summary, the distributions of Sb concentration in size-classified APM collected at both the roadside and residential sites exhibit a unique bimodal profile. Moreover, several similar profiles of size distributions for Cu, Ba, Cd, and Pb, which are probably related to the atmospheric behaviour of Sb, were observed. The similarities in these size distributions and elemental compositions are expected to provide important clues for the identification of the predominant sources of Sb. In the following sections, the effects of predominant emission sources of Sb in APM are discussed in detail by focusing on the similarities in elemental composition, particle size, and microscopic fingerprints between the ambient APM and several potential sources.

Elemental composition in dust samples collected from potential sources of APM

To develop a well-defined and representative source profile database, it is necessary to collect as many samples as possible from potential APM sources. Table 2 lists the average compositions of 13 trace elements in significant sources of APM in Japan. The right-handmost column shows the elemental composition of SRM 2689 (coal fly ash). The measured values were in good agreement with their certified and reference values.

Extremely high concentrations of Sb (1.46%), Cu (14.6%), and Ba (12.0%) were found in the brake abrasion dusts. As stated in our previous study,[17] these three elements are good indicators of automotive brake abrasion dusts. A great number of automotive brake pads (more than 60% of commercially available brake pads in Japan) contain Sb_2S_3 as a solid lubricant to control the friction coefficient.[21] $BaSO_4$ is added to brake pads as a filler, and Cu fibre is used as an aggregate to improve the mouldability and strength of the brake pad. Therefore, brake abrasion dust is believed to be one of the most significant sources of Sb, Cu, and Ba in APM. In addition to brake abrasion dust, a high concentration of Sb (349 μg g^{-1}) was found in waste fly ash. This observation may be explained by the fact that some Sb-containing wastes such plastics and chemical fabrics are incinerated in Japan.[19] Moreover, the concentrations of potentially toxic elements such as Cd (32.7 μg g^{-1}) and Pb (2360 μg g^{-1}) were also found to be relatively high in waste fly ash compared with the other source samples. Elements having low boiling points were probably enriched on the surface of fly ash through a high-temperature incineration process.[22] The Sb concentration in coal fly ash was relatively low (8.9 μg g^{-1}). Narukawa et al.[23] measured the Sb concentrations in coal fly ash samples collected from six different coal-fired thermal power stations in several countries, and they reported that the Sb concentrations ranged from 0.79 to 3.9 μg g^{-1}, which is similar to but lower than the concentration determined in the present study. Likewise, Qi et al.[24] measured Sb concentrations in a large number of Chinese coal samples ($n = 1058$) and reported that the average concentration of Sb was ~7 μg g^{-1} (Sb concentrations found in the majority of samples ($n = 923$) were below 10 μg g^{-1}). These results suggest that coal combustion may be not so important for Sb contamination in APM in Japan compared with brake abrasion dust and waste fly ash. Moreover, the other sources investigated in the present study contained relatively low concentrations of Sb, suggesting that these sources will be less important for the emission of Sb to the atmosphere.

As indicated in Fig. 2, the relationships among Sb, Cu, Ba, Cd, and Pb can be used as the effective elemental fingerprints for the identification of the predominant sources of Sb. To compare the elemental compositions in size-classified ambient APM and those in several emission sources, the elemental ratios Cu/Sb, Ba/Sb, Cd/Sb, and Pb/Sb were calculated.

For the peaks of the coarse fraction (3.6–5.2 μm) of ambient APM, the elemental ratios of Cu/Sb and Ba/Sb were calculated to be 6.8 and 8.0 for the roadside site and 14 and 10 for the residential site, respectively. These values were similar to those calculated in brake abrasion dust (Cu/Sb, 10; Ba/Sb, 8.2; values are shown in the bottom rows in Table 2). However, for the peaks of the fine fraction (0.5–0.7 μm), the elemental ratios Cd/Sb and Pb/Sb are calculated to be 0.12 and 3.4 for the roadside site and 0.15 and 4.7 for the residential site, respectively. These values were similar to those calculated in waste fly ash (Cd/Sb, 0.094; Pb/Sb, 6.8). The elemental ratios calculated in the other sources were quite different from those for either the coarse or fine fraction of ambient APM. Consequently, in terms of the elemental fingerprints, brake abrasion dust and waste fly ash are most likely to be the predominant sources of Sb in coarse and fine ambient APM, respectively.

Distributions of elemental concentrations in size-classified brake abrasion dust and waste fly ash

To confirm the hypothesis that Sb in coarse and fine ambient APM is attributed to brake abrasion dust and waste fly ash, we determined the distributions of elemental concentrations in size-classified dust samples emitted from two potential Sb sources.

Fig. 3 illustrates the distributions of the elemental concentrations for Sb, Cu, and Ba in size-classified brake abrasion dusts emitted from selected brake pads (data are cited from ref. [17]). As discussed in detail in our previous study, the peaks of Sb, Cu, and Ba were found at ~4 μm.[17] These features are in good agreement with the peaks of Sb, Cu, and Ba observed in the coarse fractions (3.6–5.2 μm) of ambient APM (see Fig. 2). In other words, the hypothesis that brake abrasion dust dominates the peak of Sb in coarse fractions of APM is also strongly supported by the size distribution of elemental concentration in brake abrasion dust.

Fig. 4a illustrates the distributions of elemental concentrations (ng m^{-3}) for Sb, Cd, and Pb obtained by re-entrainment examination of waste fly ash. The peaks of these elements were observed at ~2 μm (other measured elements also showed similar distributions). A similar result was obtained from APS

Table 2. Elemental concentrations and ratios of significant sources of airborne particulate matter (APM) in Japan

Concentration data ranges are listed following the average values in parentheses (minimum, maximum). Brake abrasion dust data are cited from ref. [17]. SRM 2689 (coal fly ash) prepared by National Institute of Standards and Technology (NIST) was measured. Elemental ratio values were calculated from average concentrations. N.D., not detected; and N.M., not measured

Element	Concentration ($\mu g\,g^{-1}$)						
	Waste fly ash $n=10$	Oil fly ash $n=8$	Wood fly ash $n=3$	Diesel exhaust particle (DEP) $n=3$	Soil $n=3$	Brake abrasion dust $n=3$	Coal fly ash $n=1$
V	17.5 (4.2, 53.4)	68.0 (20.4, 119)	6.8 (2.2, 10.7)	192 (8.1, 429)	196 (160, 254)	N.M.	307
Cr	660 (44.6, 4430)	202 (N.D., 679)	52.6 (10.7, 98.5)	53.0 (N.D., 121)	65.9 (31.6, 93.9)	N.M.	167
Mn	332 (7.2, 784)	53.0 (N.D., 369)	344 (127, 567)	N.D.	1060 (756, 1340)	N.M.	295
Ni	678 (14.5, 3550)	5.8 (N.D., 25.1)	0.8 (N.D., 2.5)	66 (N.D., 199)	32.6 (17.6, 41.9)	N.M.	129
Cu	868 (3.5, 3600)	49.5 (N.D., 182)	118 (79.7, 159)	3.1 (N.D., 9.2)	97.5 (49.3, 139)	146 000 (99 000, 210 000)	131
Zn	11 900 (223, 34 500)	N.D.	2820 (1220, 4670)	887 (N.D., 1940)	231 (90.7, 330)	10 200 (630, 29 000)	253
As	11.3 (0.9, 23.2)	6.7 (N.D., 19.0)	18.3 (13.6, 27.5)	0.7 (N.D., 2.1)	8.1 (7.4, 9.0)	N.D.	139
Se	0.7 (N.D., 5.1)	0.1 (N.D., 0.3)	N.D.	2.0 (N.D., 6.1)	0.7 (0.6, 0.8)	N.D.	7.4
Mo	128 (9.3, 404)	33.1 (N.D., 150)	14.1 (0.6, 33.0)	64.6 (N.D., 155)	1.9 (1.5, 2.6)	N.M.	37.5
Cd	32.7 (0.1, 111)	5.8 (0.2, 36.5)	5.7 (1.6, 9.6)	0.1 (N.D., 0.2)	0.5 (0.3, 0.7)	N.D.	2.6
Sb	349 (1.0, 972)	10.4 (0.7, 20.7)	10.7 (6.8, 17.3)	1.1 (N.D., 3.3)	2.4 (0.8, 3.3)	14 600 (7800, 19 000)	8.9
Ba	1290 (308, 2550)	N.M.	N.M.	N.M.	243 (190, 335)	120 000 (81 000, 140 000)	732
Pb	2360 (17.4, 5750)	79.0 (N.D., 282)	247 (134, 395)	N.D.	52.5 (16.3, 84.8)	N.D.	62.1
	Elemental ratio						
Cu/Sb	2.5	4.8	11	2.8	41	10	15
Ba/Sb	3.7	–	–	–	100	8.2	100
Cd/Sb	0.094	0.56	0.54	0.057	0.22	–	0.29
Pb/Sb	6.8	7.6	23	–	22	–	6.9

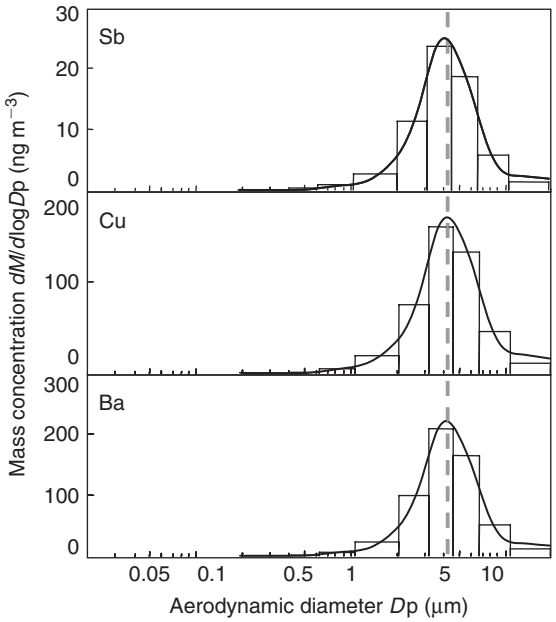

Fig. 3. Distributions of elemental concentrations in size-classified brake abrasion dust. The data are cited from ref. [17]. The solid curve indicates smoothed distribution and the broken line indicates the coarser peak diameter observed in the distribution of Sb concentration in ambient airborne particulate matter (APM).

for the total mass concentration of the fly ash. These features disagreed with those of the ambient data in terms of the size distributions (the peaks at 2 μm for waste fly ash and 0.6 μm for ambient APM) of elemental concentrations (ng m^{-3}). Then, the geometrical size of fly ash particles was measured using SEM. As shown in Fig. 4b, a large number of aggregated cluster particles, whose sizes are approximately several micrometres, were found. These cluster particles were typically composed of a large number of submicron-sized particles. There are two possible causes of the aggregation. One possibility is that the aggregation of submicron-sized particles might have occurred by the cooling of heated flue gas in the electric precipitator. Another possibility is that the aggregation might have occurred by the absorption of moisture during sample storage. In either case, the distributions of elemental concentrations of the waste fly ash sample obtained in the current study might have been shifted to the coarser side compared with the original one owing to the aggregation of individual particles. This suggests that direct collection from the flues is required in order to obtain an accurate particle size distribution. Although a geometric diameter (obtained from the SEM image) is not the same as an aerodynamic diameter (depicted in Figs 2 and 4a), microscopic observations indicated that the waste fly ash was originally composed of submicron-sized particles. We then converted the unit of elemental concentration from ng m^{-3} to μg g^{-1} (see Fig. 4c) in order to focus on the elemental composition in the fine fractions. Sb, Cd, and Pb are slightly enriched in the fine fractions (0.3–0.5 μm and 0.5–0.7 μm) compared with those in the other fractions, confirming that Sb, Cd, and Pb can be considered as the marker elements in the submicron-sized waste fly ash. Elemental ratios of Cd/Sb and Pb/Sb in respective size fractions were calculated and are shown in Fig. 4d. Cd/Sb ratios in respective fractions tended to increase with decreasing particle size. As a result, Cd/Sb ratios in the fine fractions became higher than that in the bulk composition, whereas Pb/Sb ratios tended to decrease with decreasing particle size. This caused the Pb/Sb ratios in the fine fractions to become lower than that in the bulk composition. Consequently, the abovementioned elemental fractionations will largely contribute to the elemental ratios of submicron-sized ambient APM. Although we have no obvious causes other than the differences in melting and boiling points among the elements, the occurrence of the aforementioned elemental fractionation may cause some uncertainties for source identification of size-classified APM.

Microscopic fingerprint of Sb-enriched ambient APM

Fig. 5a shows an SEM image and elemental distribution images obtained from EDX spectra of Sb (Lα1 line) and S (Kα1 line) existing in the coarse fraction (3.6–5.2 μm) of the roadside APM. Considering the detection limits of SEM-EDX, substantial EDX signals are supposed to be obtained for the elements whose concentrations are more than of subpercentage order. As shown in Fig. 5a, particles containing Sb are easily found among the roadside APM. Large parts of Sb images resembled the S images, indicating that there exists a large amount of particles that are composed of Sb and S in the coarse fraction of APM. Moreover, the shapes of such particles were typically angular-shaped, which implies these particles were generated by mechanical abrasion (we described the morphology of angular-shaped as square-shaped in our previous paper[12]). These microscopic fingerprints are very similar to those of brake abrasion dust (see Fig. 5b). Because Sb_2S_3 is used for brake pads, lots of particles with high concentrations of Sb and S will be found by microscopic observation. Although strong signals of Ba and Cu were also found in some brake abrasion dust particles, those elemental images did not coincide with that of Sb because brake pads are composed of various raw materials. Consequently, the hypothesis that brake abrasion dust dominates the peak of Sb in coarse fractions of APM is also strongly supported by the microscopic fingerprints.

Despite the high concentration of Sb in the fine fraction (0.5–0.7 μm), it was difficult to find particles containing Sb among the APM in fine fraction in the residential site as shown in the upper images in Fig. 5c. Likewise, particles containing Sb could not be found among the fine APM in the roadside site. The lower images in Fig. 5c show one of the examples in which significant EDX signals of Sb and S were detected from identical particles. For comparison, microscopic images of waste fly ash are shown in Fig. 5d. As shown in Fig. 5d, although strong EDX signals of Sb and S can be detected in waste fly ash, their elemental distribution images are not identical. This implies that volatilised Sb probably condensed on the surface of fly ash particles, which will be separate from sulfur compounds. The different microscopic fingerprints shown in Fig. 5c, d indicate that the particles containing Sb (shown in Fig. 5c) may not have been emitted from waste incinerators. However, the particles may be recognised as a brake abrasion dust in terms of the similarities in microscopic fingerprints with those shown in Fig. 5b. The sizes of most particles found in the fine fraction (see Fig. 5c) were significantly large compared with the theoretically classified particle size range (0.5–0.7 μm). A similar tendency was observed for the other finer fractions. These large particles possessed a smooth surface corresponding to the typical morphological feature of salt. Moreover, elemental distribution images indicated that the major component of these particles was S. Furthermore, considerably high concentrations of SO_4^{2-} were determined from the fine fractions by means of a complementary measurement using ion chromatography; these results indicate that the majority of

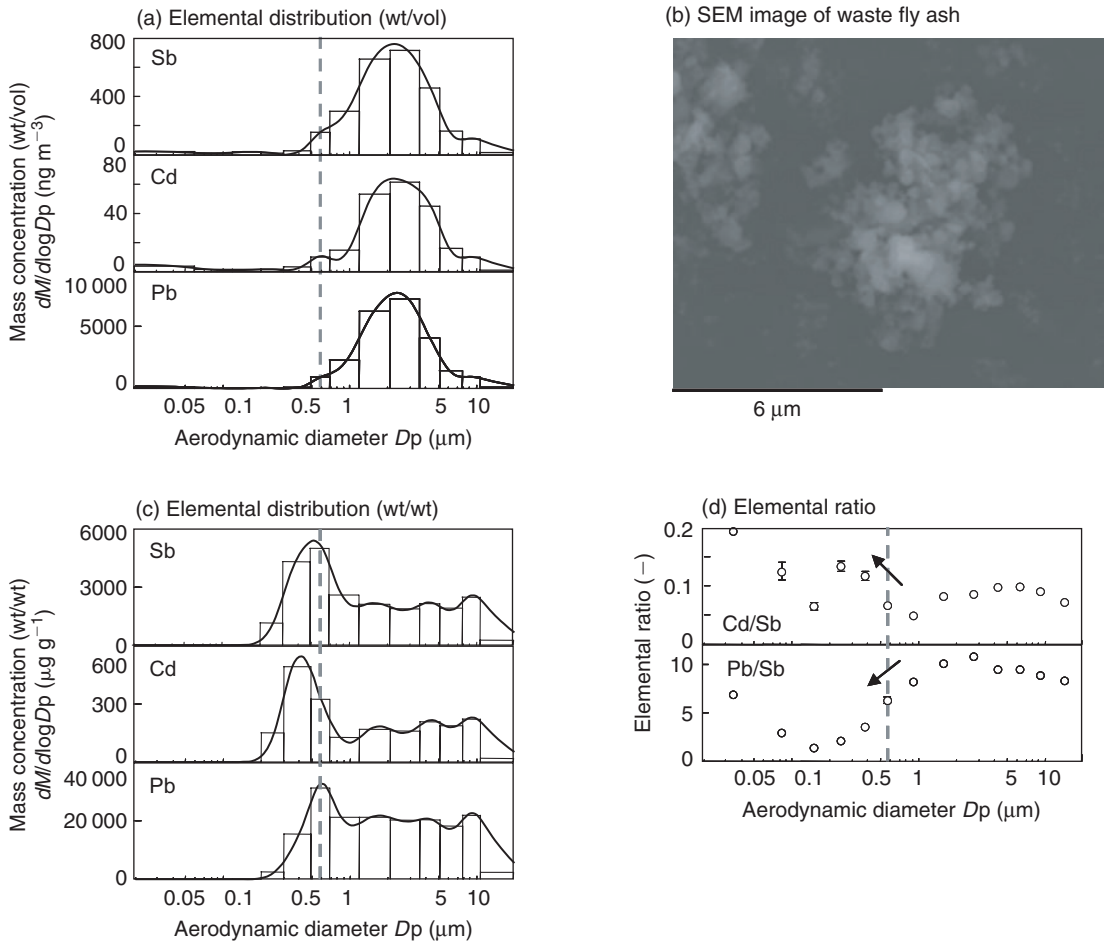

Fig. 4. Distributions of elemental concentrations and ratios in a size-classified waste fly ash sample and a typical SEM image of ash particles. The solid curve indicates smoothed distribution and the broken line indicates the finer peak diameter observed in the distribution of Sb concentration in ambient airborne particulate matter (APM). (a) Elemental distributions in units of ng m^{-3}; (b) typical scanning electron microscope (SEM) image of aggregated waste fly ash before the re-entrainment examination; (c) elemental distributions in units of μg g^{-1}; and (d) elemental ratios in size-classified waste fly ash. The error bars in (d) indicate ±standard deviations.

these large particles were sulfate and that they were probably condensed and produced on the surface of the originally collected fine particles during sample collection. Considering the above assumption, the reason for not obtaining a large number of fine particles containing Sb can be interpreted, because the original fine particles were covered with a thick sulfate layer. To elucidate this phenomenon, the internal composition of a particle must be measured with high sensitivity. To this end, some advanced analytical techniques such as secondary ion mass spectrometry (SIMS)[25] will be required.

Source apportionment to Sb in size-classified ambient APM by chemical mass balance analysis

In the previous sections, the potential sources of Sb in size-classified APM were qualitatively discussed by means of the comparisons of elemental compositions, size distributions of elemental concentrations, and microscopic images between ambient APM and several potential sources. As a result, brake abrasion dust and waste fly ash were identified as the predominant sources of Sb in coarse and fine APM, respectively. The contributions of seven types of potential sources listed in Table 2 were apportioned to the mass concentrations of 13 elements in each size-classified APM by means of chemical mass balance (CMB) analysis. A description of the CMB model is given in our previous study.[13]

The mass concentration of 13 elements apportioned to respective sources were found to be in good agreement with the field observation values ($r^2 = \sim 0.7$), indicating that the database of elemental composition for seven types of potential sources sufficiently represented the emission sources of ambient APM. Fig. 6 illustrates the source apportionment to Sb in the size-classified APM. Brake abrasion dust and waste fly ash dominated the large portions of Sb in the size-classified APM in both the sites. In particular, brake abrasion dust dominated the Sb in the coarser fractions, whereas the waste fly ash dominated that in the finer fractions. These results are consistent with the qualitative discussions described above. Coal fly ash, which is considered to be a significant Sb source in the world,[11] accounted for less contribution in the sites studied, suggesting that it may not be a significant source of Sb in Japan.

At the roadside site, the contributions of brake abrasion dust and waste fly ash accounted for 55% (2.0 ng m^{-3}) and 38% (1.4 ng m^{-3}) of the total observed Sb concentration (3.7 ng m^{-3}), respectively. At the residential site, the contributions of brake abrasion dust and waste fly ash accounted for

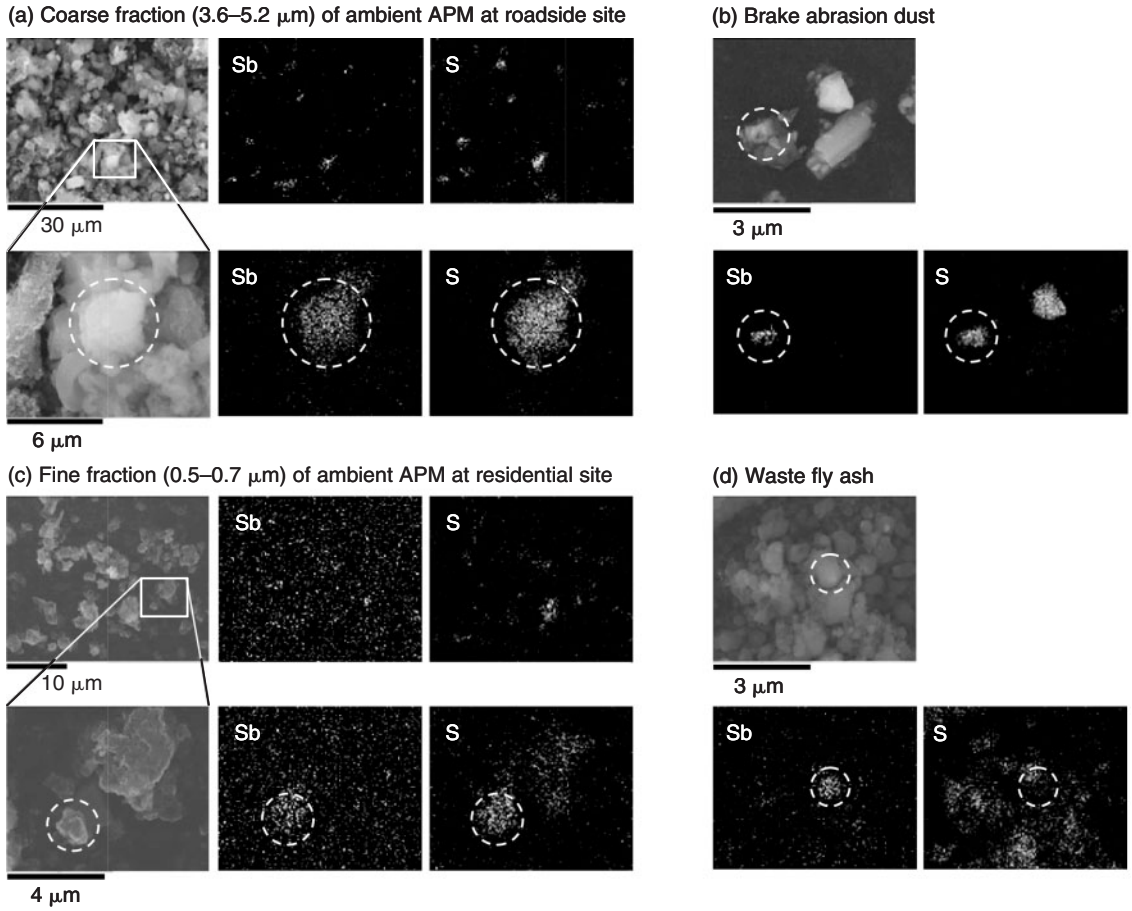

Fig. 5. Microscopic images of ambient airborne particulate matter (APM) and potential sources. (a) Coarse fraction of ambient APM at the roadside site; (b) brake abrasion dust; (c) fine fraction of ambient APM at the residential site; and (d) waste fly ash.

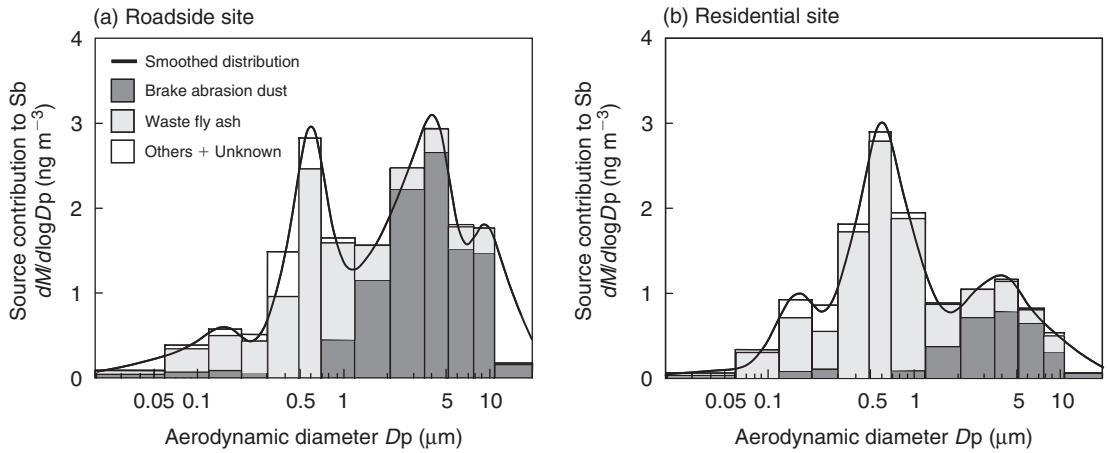

Fig. 6. Source contributions of brake abrasion dust and waste fly ash to Sb in size-classified ambient airborne particulate matter (APM) collected at (a) the roadside site and (b) the residential site.

24% (0.6 ng m^{-3}) and 68% (1.8 ng m^{-3}) of the total observed Sb concentration (2.7 ng m^{-3}), respectively. These quantitative evaluations imply that the concentration of Sb in APM is dominated by these two sources and that the effects of respective sources on Sb concentrations vary depending on the location of the investigation site. The data obtained in the current study are also useful to discuss the magnitude of the circulation of airborne Sb. As the residence time of coarse APM is short, the contribution of brake abrasion dusts might be limited to a local scale. However, waste fly ash particles may potentially affect the contamination of Sb on a global scale because the residence time of fine APM is relatively long. These findings will partly contribute to understanding the cycles and fates of Sb from both the local and global viewpoints.

Conclusion

A characteristic bimodal profile was found in the distribution of Sb concentration in size-classified APM. By focusing on the elemental composition, size distributions of elemental concentrations, and microscopic images, predominant sources of Sb were qualitatively identified. One of the sources is automotive brake abrasion dust, which has significant effect on the Sb in coarser fractions of APM. The other source is waste fly ash, which is most likely to affect the Sb in finer fractions of APM. The effects of the potential sources were quantitatively determined by means of CMB analysis. In conclusion, the concentration of Sb in APM is dominated by the above mentioned two sources, and the effects of the respective sources are specifically shown in the different size fractions of APM. This shows one case study of the effects of Sb on the atmosphere in suburbs of Tokyo, Japan, and in order to estimate the Sb inventory in Japan, further studies in other specific fields such as mega-cities and remote areas will be required.

Acknowledgement

We are grateful for the financial support provided by the Ministry of Education, Science, Sports, and Culture, Japan, through the Grants-in-Aid for scientific research (project number 19710022 and 19750064). We are also grateful to Dr Shuichi Hasegawa (National Institute for Environmental Studies), Ms Kiyoko Yano (Akebono Brake Industry Co. Ltd), Ms Kimiyo Kumagai, Ms Misato Shimoda, Dr Masahiro Fujita (Gunma Prefectural Institute of Public Health and Environmental Sciences), and Dr Hirokazu Kimura (Infectious Diseases Surveillance Center, National Institute of Infectious Diseases) for helpful discussions.

References

[1] B. Maher, Foreword: research front – arsenic biogeochemistry. *Environ. Chem.* **2005**, *2*, 139. doi:10.1071/EN05063

[2] P. G. C. Campbell, Cadmium – a priority pollutant. *Environ. Chem.* **2006**, *3*, 387. doi:10.1071/EN06075

[3] R. Ebinghaus, Mercury cycling in the Arctic – does enhanced deposition flux mean net-input? *Environ. Chem.* **2008**, *5*, 87. doi:10.1071/EN08024

[4] W. Shotyk, B. Chen, M. Krachler, Lithogenic, oceanic and anthropogenic sources of atmospheric Sb to a maritime blanket bog, Myrarnar, Faroe Islands. *J. Environ. Monit.* **2005**, *7*, 1148. doi:10.1039/B509928P

[5] W. Shotyk, M. Krachler, B. Chen, Antimony in recent, ombrotrophic peat from Switzerland and Scotland: comparison with natural background values (5320 to 8020 ^{14}C yr BP) and implications for the global atmospheric Sb cycle. *Global Biogeochem. Cycles* **2004**, *18*, GB1016. doi:10.1029/2003GB002113

[6] J. M. Cloy, J. G. Farmer, M. C. Graham, A. B. MacKenzie, G. T. Cook, A comparison of antimony and lead profiles over the past 2500 years in Flanders Moss ombrotrophic peat bog, Scotland. *J. Environ. Monit.* **2005**, *7*, 1137. doi:10.1039/B510987F

[7] M. Krachler, J. Zheng, R. Koerner, C. Zdanowicz, D. Fisher, W. Shotyk, Increasing atmospheric antimony contamination in the northern hemisphere: snow and ice evidence from Devon Island, Arctic Canada. *J. Environ. Monit.* **2005**, *7*, 1169. doi:10.1039/B509373B

[8] M. Krachler, J. Zheng, D. Fisher, W. Shotyk, Atmospheric Sb in the Arctic during the past 16 000 years: responses to climate change and human impacts. *Global Biogeochem. Cycles* **2008**, *22*, GB1015. doi:10.1029/2007GB002998

[9] J. Zheng, M. Tan, Y. Shibata, A. Tanaka, Y. Li, G. Zhang, Y. Zhang, Z. Shan, Characteristics of lead isotope ratios and elemental concentrations in PM_{10} fraction of airborne particulate matter in Shanghai after the phase-out of leaded gasoline. *Atmos. Environ.* **2004**, *38*, 1191. doi:10.1016/J.ATMOSENV.2003.11.004

[10] J. Chen, M. Tan, Y. Li, J. Zheng, Y. Zhang, Z. Shan, G. Zhang, Y. Li, Characteristics of trace elements and lead isotope ratios in $PM_{2.5}$ from four sites in Shanghai. *J. Hazard. Mater.* **2008**, *156*, 36. doi:10.1016/J.JHAZMAT.2007.11.122

[11] J. M. Pacyna, E. G. Pacyna, An assessment of global and regional emissions of trace metals to the atmosphere from anthropogenic sources worldwide. *Environ. Rev.* **2001**, *9*, 269. doi:10.1139/ER-9-4-269

[12] N. Furuta, A. Iijima, A. Kambe, K. Sakai, K. Sato, Concentrations, enrichment and predominant sources of Sb and other trace elements in size-classified airborne particulate matter collected in Tokyo from 1995 to 2004. *J. Environ. Monit.* **2005**, *7*, 1155. doi:10.1039/B513988K

[13] A. Iijima, H. Tago, K. Kumagai, M. Kato, K. Kozawa, K. Sato, N. Furuta, Regional and seasonal characteristics of emission sources of fine airborne particulate matter collected in the center and suburbs of Tokyo, Japan, as determined by multielement analysis and source receptor models. *J. Environ. Monit.* **2008**, *10*, 1025. doi:10.1039/B806483K

[14] Y. Gao, E. D. Nelson, M. P. Field, Q. Ding, H. Li, R. M. Sherrell, C. L. Gigliotti, D. A. Van Ry, T. R. Glenn, S. J. Eisenreich, Characterization of atmospheric trace elements on $PM_{2.5}$ particulate matter over the New York–New Jersey harbor estuary. *Atmos. Environ.* **2002**, *36*, 1077. doi:10.1016/S1352-2310(01)00381-8

[15] G. Weckwerth, Verification of traffic-emitted aerosol components in the ambient air of Cologne (Germany). *Atmos. Environ.* **2001**, *35*, 5525. doi:10.1016/S1352-2310(01)00234-5

[16] D. R. Gómez, M. F. Giné, A. C. S. Bellato, P. Smichowski, Antimony: a traffic-related element in the atmosphere of Buenos Aires, Argentina. *J. Environ. Monit.* **2005**, *7*, 1162. doi:10.1039/B508609D

[17] A. Iijima, K. Sato, K. Yano, H. Tago, M. Kato, H. Kimura, N. Furuta, Particle size and composition distribution analysis of automotive brake abrasion dusts for the evaluation of antimony sources of airborne particulate matter. *Atmos. Environ.* **2007**, *41*, 4908. doi:10.1016/J.ATMOSENV.2007.02.005

[18] A. Iijima, K. Sato, K. Yano, M. Kato, K. Kozawa, N. Furuta, Emission factor for antimony in brake abrasion dusts as one of the major atmospheric antimony sources. *Environ. Sci. Technol.* **2008**, *42*, 2937. doi:10.1021/ES702137G

[19] K. Tsunemi, H. Wada, Substance flow analysis of antimony for risk assessment of antimony and antimony compounds in Japan. *J. Japan Inst. Metals* **2008**, *72*, 91. doi:10.2320/JINSTMET.72.91

[20] N. S. Mokgalaka, R. I. McCrindle, B. M. Botha, Multielement analysis of tea leaves by inductively coupled plasma optical emission spectrometry using slurry nebulisation. *J. Anal. At. Spectrom.* **2004**, *19*, 1375. doi:10.1039/B407416E

[21] H. Jang, S. J. Kim, The effects of antimony trisulfide (Sb_2S_3) and zirconium silicate ($ZrSiO_4$) in the automotive brake friction material on friction characteristics. *Wear* **2000**, *239*, 229. doi:10.1016/S0043-1648(00)00314-8

[22] S. Jiménez, M. Pérez, J. Ballester, Vaporization of trace elements and their emission with submicrometer aerosols in biomass combustion. *Energy Fuels* **2008**, *22*, 2270. doi:10.1021/EF800111U

[23] T. Narukawa, A. Takatsu, K. Chiba, K. W. Riley, D. H. French, Investigation on chemical species of arsenic, selenium and antimony in fly ash from coal fuel thermal power stations. *J. Environ. Monit.* **2005**, *7*, 1342. doi:10.1039/B509817C

[24] C. Qi, G. Liu, C.-L. Chou, L. Zheng, Environmental geochemistry of antimony in Chinese coals. *Sci. Total Environ.* **2008**, *389*, 225. doi:10.1016/J.SCITOTENV.2007.09.007

[25] C. Font Palma, G. J. Evans, R. N. S. Sodhi, Imaging of aerosols using time of flight secondary ion mass spectrometry. *Appl. Surf. Sci.* **2007**, *253*, 5951. doi:10.1016/J.APSUSC.2006.12.126

Manuscript received 13 December 2008, accepted 12 February 2009

Appendix. Analytical results of National Institute of Standards and Technology (NIST) SRM 1648

Element	NIST SRM 1648 (Urban particulate matter)		
	Found[A] ($\mu g\,g^{-1}$)	Certified or reference[B] ($\mu g\,g^{-1}$)	Recovery (%)
V	130 ± 4	127	102
Cr	400 ± 24	403	99
Mn	778 ± 34	786	99
Ni	66.0 ± 1.2	82	80
Cu	563 ± 45	609	92
Zn	4780 ± 148	4760	100
As	114 ± 3	115	99
Se	24.7 ± 1.1	27	91
Mo	14.6 ± 0.6	–	–
Cd	71.8 ± 4.4	75	96
Sb	42.7 ± 1.5	45[B]	95
Ba	702 ± 20	737[B]	95
Pb	6650 ± 156	6550	102

[A]Values were derived from the analysis of three samples.
[B]Reference value.